Sensitivity, Resolution and Image Quality with a Multi-Head SPECT Camera

Frederic H. Fahey, Beth A. Harkness, John W. Keyes, Jr., Mark T. Madsen, Christina Battisti, and Valerie Zito

Georgetown University Hospital, Department of Radiology, Division of Nuclear Medicine, Washington, DC and the University of Iowa School of Medicine, Department of Radiology, Iowa City, Iowa

This investigation sought to determine which collimation factors were most important in providing superior image quality with a three-headed SPECT device. The relationship between sensitivity, resolution and SPECT image quality was studied. Two different sets of parallel-hole collimators were used. The ultrahigh-resolution collimators have higher spatial resolution (8.9 versus 11.0 mm), but only 55% of the sensitivity of the high-resolution collimators. A phantom with hot rods was imaged with both collimator sets. Observers compared images with the ultrahigh-resolution collimators to images of varying counts with the high-resolution collimators and determined which high-resolution images matched the ultrahigh-resolution images in image quality. Eleven patient studies were acquired with both collimator sets for equal time, and observers chose which image set they preferred. Transverse images of brain and liver studies were simulated with varying resolution and counts and subjectively compared. The phantom study indicated that the improvement in resolution led to image quality comparable to increasing the number of counts by a factor of 2.5 to 3.4. The clinical studies showed that the ultrahigh-resolution collimators were preferred in a large majority of the cases. These trends were also seen in the simulation study. These results confirm that higher resolution collimators should be used with multihead SPECT devices. The improvement in resolution more than compensates for the loss in sensitivity, leading to an overall improvement in image quality.

J Nucl Med 1992; 33:1859–1863

In nuclear medicine, the choice of collimator involves a tradeoff between sensitivity and spatial resolution. Although the same can be said for single-photon emission computed tomography (SPECT), the choice of the most appropriate collimator is not always obvious. Muehllehner reported on a study where he simulated emission computed tomography images of the Derenzo phantom by varying the spatial resolution and the total number of counts (*1*). Observers were asked to match images of similar image quality. An improvement in resolution of 2 mm (e.g., from 10 mm to 8 mm) required only about one-fourth as many counts for comparable image quality. In the range of spatial resolutions normally encountered in clinical SPECT, an improvement of 2 mm does not cost a factor of four in counts, but more typically less than a factor of two, indicating that one should use higher resolution collimators for the best SPECT image quality.

These results are based upon the simulated data of a particular phantom (the Derenzo phantom). Such results might depend upon the simulation model used to simulate the imaging device and the object being imaged. Actual SPECT images have varying spatial resolution and noise characteristics across the transverse field of view, due to such effects as collimator response, attenuation and scatter. In clinical SPECT, the objects being imaged vary greatly in their signal content. In addition, the contrast may not only vary between images but within the same image. These clinical images may also have structures that are not as readily recognizable as in the Derenzo phantom, and thus the observer may have more difficulty in discerning real structures from noise. For these reasons, we sought to determine if the conclusions drawn from Muehllehner's data were true with actual SPECT data. His experiment was replicated with actual SPECT phantom data, and a study was performed that compared clinical images acquired with two collimator sets. In addition, simulated clinical images and an objective measure of image quality, the normalized mean square error, were used to evaluate the effect of sensitivity and resolution on SPECT image quality.

METHODS

All of the studies in this investigation were acquired with a three-headed, rotating camera dedicated to SPECT (Triad, Trionix Research Laboratories, Twinsburg, OH). In this investigation, we compared two sets of collimators provided with the Triad: low-energy, high-resolution and low-energy, ultrahigh-resolution. Table 1 compares the two collimator sets with respect to tomographic spatial resolution and sensitivity. The tomographic resolution was evaluated by placing a capillary tube in the center of the Jaszczak phantom (Data Spectrum Corp, Chapel Hill, NC) and imaging it with a radius of rotation of 14.5 cm with 120 angles over 360°. The projection data were then reconstructed with a ramp filter and the full width at half maximum (FWHM) across the resultant image was determined. The sensi-

Received Sept. 27, 1991; revision accepted Jun. 2, 1992.

For reprints contact: Frederic H. Fahey, DSc, PET Center, Bowman Gray School of Medicine, Medical Center Blvd., Winston-Salem, NC 27157-1061.

TABLE 1
Collimators for the Trionix TRIAD

Collimator set	Tomographic resolution (mm)	Relative planar sensitivity
High-resolution	11.0 mm	1.00
Ultrahigh-resolution	8.9 mm	0.55

The tomographic resolution was determined by imaging a capillary tube (filled with ^{99m}Tc) at the center of the Data Spectrum phantom, located near the axis of rotation. The radius of rotation was 14.5 cm and the 120 images were acquired over 360° and reconstructed with a ramp filter. The relative sensitivity was determined by acquiring a 1 minute count of 1 mCi of ^{99m}Tc in a culture flask (10 × 10 cm) on the collimator face.

tivity was determined by counting a small area source (10 × 10 cm culture flask) for 60 sec with both collimator sets and reporting the results relative to the sensitivity of the high-resolution collimators.

We performed a phantom study to see if Muehllehner's results were consistent with actual SPECT data. The Jaszczak phantom with Deluxe hot rods was used. Eight images were acquired with the high-resolution collimator (HR1–HR8) with varying counts such that HRn had n times as many counts as HR1 (e.g., HR4 has four times as many counts as HR1). In addition, three images were acquired with the ultrahigh-resolution collimators (UR1–UR3). UR1 was acquired for the same time as HR1, UR2 for the same time as HR2, and UR3 for the same time as HR4. All images were acquired into a 128 × 128 matrix (pixel size 3.56 mm) and reconstructed with a Hamming filter and a cutoff frequency of 1.0 Nyquist. A typical display of the phantom data is shown in Figure 1 with the eight high-resolution images at the top and the ultrahigh-resolution image at the bottom. Seven observers were asked to compare the ultrahigh-resolution image to the set of high-resolution images (HR1–HR8) and to determine which high-resolution image matched the ultrahigh-resolution image with respect to image quality. This test was repeated for each of the three ultrahigh-resolution images. An "estimated" comparable high resolution image was then calculated based on the mean of the choices of all observers.

A study was also performed that compared patient studies acquired with the two collimator sets. Eleven patient studies (eight ^{99m}Tc-HMPAO brain scans, three ^{99m}Tc-sulfur colloid liver scans) have been performed with both collimator sets. The two studies were acquired sequentially for an equal time (corrected slightly to compensate for radioactive decay). The liver scans were acquired into 128 × 128 matrices, whereas the brain scans were acquired into 64 × 64 matrices with a factor of two zoom, thus all scans had 3.56 mm pixel size. The reconstruction filter was a Hamming filter with a 1.2 and 1.0 cycles/cm cutoff frequency for the brain and liver studies, respectively. Figure 2 shows comparable slices of a liver and a brain scan acquired with each collimator set.

Four or five observers (three board certified nuclear medicine physicians and two nuclear medicine fellows with at least one year experience) were presented with full sets of comparable, transverse slices acquired with each collimator set and asked to determine which image set they preferred, without knowing which image set was acquired with which collimator set.

A simulation study was performed to obtain some insight into these phantom and clinical study results. Transverse images of the single-slice Hoffman brain phantom and a simulated liver-spleen scan were generated into a 256 × 256 matrix. Projection image sets were generated from these data which varied with respect to noise (total counts) and system resolution. These data were reduced to 128 projection bins. The system resolution varied from 7 to 13 mm for the brain image and 10 to 17 mm for the

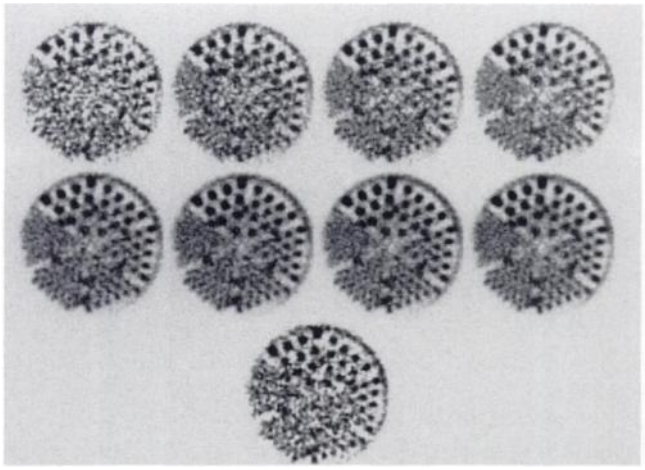

FIGURE 1. An example of the presentation used for the phantom study. The eight images at the top were acquired with the high-resolution collimators for varying numbers of counts. The bottom image was acquired with the ultrahigh-resolution collimators. In this example, the ultrahigh-resolution image was acquired for the same time as high-resolution image 2. Seven observers were asked to choose which high-resolution image matched the ultrahigh-resolution image with respect to image quality.

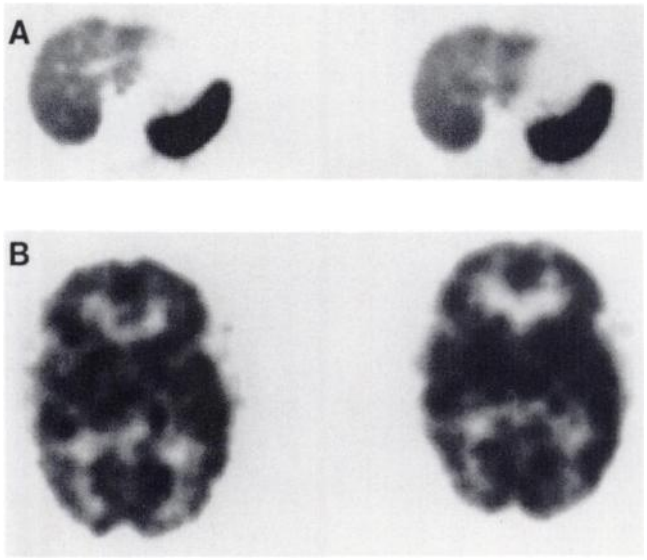

FIGURE 2. Examples from the clinical study. The two images on the right were acquired with the high-resolution collimators and those on the left with the ultrahigh-resolution. For each clinical case, both image sets were acquired for the same time (correcting slightly for radioactive decay) and the data were reconstructed with the same filter. Observers were presented with a complete set of transverse images for each set and asked to choose the image set they preferred.

liver scan. The number of counts for a typical slice using the ultrahigh-resolution collimator was determined for both the brain and liver and the counts for the other simulations were scaled according to the square of the system spatial resolution. The projection images were filtered using the smoothing portion of the Wiener filter (and not the resolution recovery portion). The filter, WFs(f), is described by the equation:

$$WFs(f) = \frac{S(f)}{S(f) + Sn(f)},$$

where f is spatial frequency, S(f) is the ideal (without noise) signal power of the object being filtered and Sn(f) is the noise power (*2*). This is an optimal filter that adapts the cutoff frequency and the nature of the filter roll-off to the content of the signal and noise for a particular image. It thus seeks to maximize the signal-to-noise of a particular image. The data were then reconstructed with a ramp filter.

The reconstructed images for each study type were then normalized to the same total "counts." The normalized mean square error (NMSE), as described by Penney et al. (*3*), was then used as an objective measure of image quality. The NMSE is given by:

$$NMSE = \frac{\sum_{i,j} \left(R(i, j) - T(i, j) \right)^2}{\sum_{i,j} \left(T(i, j) \right)^2},$$

where R(i, j) and T(i, j) are the observed (blurred and noisy) data and the ideal data, respectively. It has been shown that NMSE corresponds well to observer preference with respect to SPECT image quality (*4*).

RESULTS

The phantom study results are summarized in Table 2. The table lists the counts in each of the three ultrahigh-resolution images and the mean and standard deviation of the high-resolution image. From the mean high-resolution image number, the counts in the matched high-resolution image were estimated. The ratio of these estimated counts and the counts in the ultrahigh-resolution image was used to determine the apparent count gain factor associated with the ultrahigh-resolution collimators. In Table 2, the range of the apparent count gain factors is 2.5 to 3.4 for the three ultrahigh-resolution images. In other words, 2.5 to 3.4 more counts are necessary with the high-resolution collimators to obtain image quality comparable to that with the ultrahigh-resolution collimators.

Table 3 summarizes the patient study results. The second column indicates the number of observers who preferred the images acquired with the ultrahigh-resolution collimators, and the third column indicates the number of those preferring the high-resolution collimators. The fourth column represents the proportion of observers who preferred the ultrahigh-resolution collimators. For the liver studies, the results were unanimous. For all three studies and all five observers, the ultrahigh-resolution images were chosen in every case. For the brain studies, the mean fraction of observers preferring the ultrahigh-resolution images was 0.67 ± 0.06, which was significantly greater than 0.5 ($p < 0.01$). Although there was a general preference for the ultrahigh-resolution images, the observers took more time in deciding which images they preferred and were not as sure of their choice.

The results of the simulation studies are plotted in Figure 3. Since the NMSE is a function of the total counts within the image, the brain and liver results need to be plotted on different scales. Relative units were used for the

TABLE 2
Phantom Study Results

Ultrahigh-resolution image	1	2	3
High-resolution counts	130K	260K	510K
Mean of high-resolution image with equal imaging quality	2.1 ± 0.4	3.5 ± 0.4	6.2 ± 0.6
Estimated counts in selected high-resolution image	440K	730K	1280K
Count gain of ultrahigh-resolution	3.4	2.8	2.5

Images were acquired with the ultrahigh-resolution and the high-resolution collimators. Seven observers were shown one ultrahigh-resolution image and eight high-resolution images (with varying counts) and were asked to choose the high-resolution image that matched the ultrahigh-resolution image with respect to image quality. This was repeated for three ultrahigh-resolution images. The count gain factor for the ultrahigh-resolution collimators represents how many more counts (2.5–3.4) were necessary with the high-resolution collimators to yield an image quality comparable to that of the ultrahigh-resolution collimators.

TABLE 3
Patient Study Results

Study	Preferring ultrahigh-resolution	Preferring high-resolution	Fraction preferring ultrahigh-resolution
Brain 1	2	3	0.40
Brain 2	3	2	0.60
Brain 3	4	1	0.80
Brain 4	3	2	0.60
Brain 5	3	1	0.75
Brain 6	4	0	1.00
Brain 7	3	1	0.75
Brain 8	2	2	0.50
Liver 1	5	0	1.00
Liver 2	5	0	1.00
Liver 3	5	0	1.00

Eleven patient studies were reviewed by four or five observers. The observers were shown full sets of transverse images acquired with both the ultrahigh-resolution and high-resolution collimators and were asked to select the images they preferred without knowing which image set was acquired with which collimator. Columns 2 and 3 show the number of observers preferring the ultrahigh-resolution and high-resolution collimators, respectively. Column 4 shows the fraction preferring ultrahigh-resolution collimators.

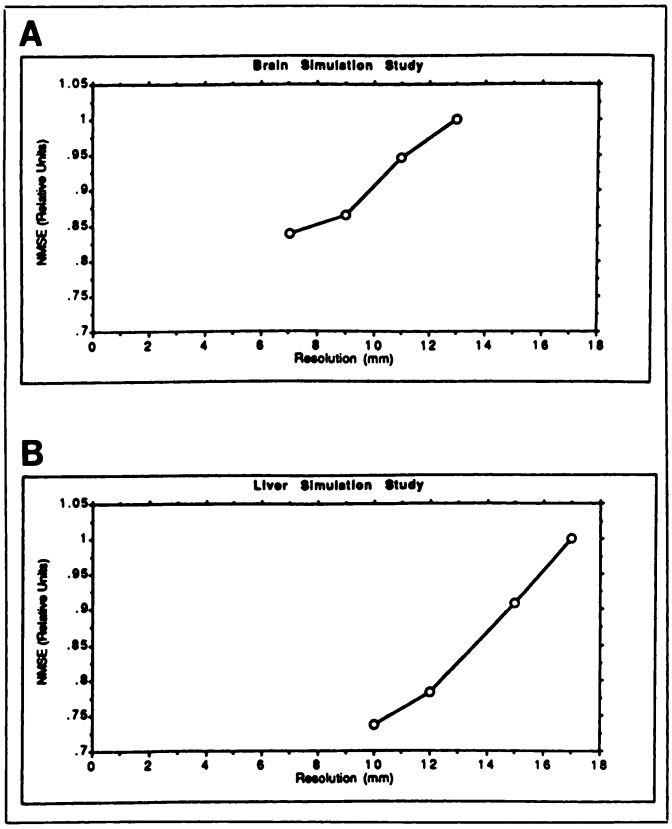

FIGURE 3. Results of the simulation study. (A) Brain results and (B) liver results. In each study, the normalized mean square error (NMSE) is plotted against the system resolution (not including the effects of the reconstruction filter). Reduced NMSE indicates improved image quality. The high-resolution and ultrahigh-resolution collimators are represented by 11 and 8 mm on the brain curve (A) and by 15 and 12 mm on the liver curve (B), respectively. Each curve was normalized to its highest NMSE value.

NMSE, normalizing to the highest value on the graph. Smaller NMSE values indicate a more accurate representation of the original data and presumably better image quality. When the resolution is low, the NMSE is high because the image is blurry and when the resolution is too high the NMSE is high because the image is noisy. An optimum lies somewhere in the middle. For the resolutions evaluated, the NMSE is reduced with improving resolution, indicating improved image quality. The high-resolution and the ultrahigh-resolution collimator are represented by 11 and 9 mm on the brain curve and 15 and 12 mm on the liver data, respectively. Notice that the relative improvement in NMSE as we go from high-resolution to ultrahigh-resolution is greater for the liver study than the brain study, matching our observations from the clinical data.

DISCUSSION

Various aspects of the choice of collimators for SPECT imaging have been studied over the years. A number of groups have investigated which collimators are most appropriate for imaging radiopharmaceuticals based on ^{123}I, produced by both the (p, 2n) and (p, 5n) reactions (*5–10*). Others have compared the use of high-resolution, long-bore collimators to conventional collimators with respect to their impact on SPECT image quality. Kirkos et al. discussed the importance of maintaining high resolution at depth in SPECT through the use of long-bore collimation (*11*). Mueller et al. compared the use of long-bore, high-resolution collimators to low-energy, general-purpose collimators and determined that the increase in resolution outweighs the increased noise due to lost sensitivity (*12*). They concluded that higher resolution collimators should yield substantial improvements in brain SPECT image quality despite a loss in counts due to the reduced collimator sensitivity. They noted work by Hanson that indicated that in the presence of unknown or varying background structure, the observer relies more heavily on high frequency information (*13*). On the other hand, Tsui et al. reported that in planar imaging the optimal resolution was on the order of the size of the lesion one is trying to evaluate (*14–16*). For clinical tasks such as liver SPECT, one might then assume that a collimator with higher sensitivity would be more appropriate.

Muehllehner's simulations indicated that one should choose higher resolution collimators (*1*). His choice of object, simulated images of the Derenzo phantom, yielded high contrast images of objects well understood by his observers. It was shown by Phelps et al. that improving the intrinsic resolution without changing the reconstruction filter or the total number of counts in simulated positron emission tomography (PET) images led not only to improved resolution within the images but also improved signal to noise (*17,18*). This increased signal-to-noise, referred to as "signal amplification," is due primarily to improved contrast of structures that are on the order of (or smaller than) the resolving capacity of the device. This is based on a reasonable model for high resolution PET where the use of small detectors leads to improved resolution with only small losses in sensitivity. In SPECT, improvement in resolution leads to losses in sensitivity proportional to the square of the FWHM. The fundamental question then becomes, "Is the improvement in contrast seen by Phelps et al. and Muehllehner enough to overcome the increased noise caused by the loss in sensitivity?" This investigation sought to validate these published results from simulation studies with actual SPECT phantom and clinical data.

The results of our phantom study are consistent with those of Muehllehner. A switch from the high-resolution to the ultrahigh-resolution collimators (improvement in resolution of about 2 mm) led to an improvement in image quality that would have required an increase in the number of counts by a factor of 2.5 to 3.4. This is similar to Muehllehner's factor of four. The difference in our values relative to Muehllehner's is most likely due to the inclusion of scatter into the true data, reducing the en-

hancement of contrast from the improved resolution. These results still indicate that improving the resolution is more efficient than improving the sensitivity with respect to image quality, since in the range of spatial resolutions normally encountered in clinical SPECT improvement in resolution by 2 mm does not cost a factor of three in counts but only about a 40%–45% loss.

The patient studies also indicate the value of improving resolution. The liver data indicate a clear preference for the ultrahigh-resolution collimators. The brain results were a bit more subtle but still implied an overall improvement in image quality. The difference in response to these two stimuli can be understood in the context of the simulation study results. The liver studies and the brain studies differ in two major ways. First, the liver studies typically contain large cold spots in a hot background, whereas the brain studies involve various structures of differing sizes and contrasts. Second, the total counts in the liver study are typically higher than for the brain studies. Since the brain images tended to be noisy, a sharp yet noisier image may confound the observer who can have difficulty separating noise from real structure, thus leading to only a moderate perceived improvement in image quality. In the liver studies, the improved resolution led to improved contrast of the vascular structures within the liver, which was deemed preferable by all observers.

Recently, Madsen et al. performed a simulation study using the Hoffman single-slice brain phantom and the NMSE as an objective measure of image quality (*4*). They compared these results with the subjective ranking of image quality by trained observers. They found that NMSE is a good indicator of image preference. They also found that the choice of collimator not only depends upon the signal content of the object being imaged, but also on the total counts within the image. Whereas Muehllehner's results tended to indicate a continuous improvement in image quality with improving resolution, Madsen's results indicated that there was an optimum resolution (leading to a minimum NMSE). This optimum resolution value shifted to lower FWHM values as the total number of counts in the study were increased.

For both the brain and liver simulation studies, the NMSE values decreased with improving resolution. However, the slope of the two curves indicates that the improvement is greater for the liver study than for the brain. These results coincide with the patient study results.

It should be noted that the criterion used in the clinical study was image preference by trained nuclear medicine physicians. A more appropriate criterion would be the accuracy of diagnosis as determined from an observer performance evaluation using receiver operator characteristic analysis. These studies, however, are very difficult to perform and require a large data set in which the true diagnosis has been obtained through a test that is considered a "gold standard." Lacking such difficult-to-obtain data, it is reasonable to assume that improving the perception of image quality is, in and of itself, a desirable outcome. The results from this study are clear cut and in good agreement with the simulation and phantom studies as well as with other published data.

We conclude that for high-quality SPECT, one should use higher resolution collimators in preference to higher sensitivity collimators when a choice can be made. The improved contrast of small structures when using the higher resolution collimators more than compensates for the increase in noise due to the loss in sensitivity, leading to an overall improvement in image quality.

REFERENCES

1. Muehllehner G. Effect of resolution on required count density in ECT imaging: a computer simulation. *Phys Med Biol* 1985;30:163–173.
2. Madsen MT. A method for obtaining an approximate Wiener filter. *Med Phys* 1990;17:126–130.
3. Penney BC, King MA, Schwinger R, et al. Constrained least-squares restoration of nuclear medicine images: selecting the coarseness function. *Med Phys* 1987;14:849–858.
4. Madsen MT, Chang W, Hichwa RD. Spatial resolution and count density requirements in brain SPECT imaging. *Phys Med Biol* 1992:in press.
5. Coleman RE, Greer KL, Drayer BP, Albright RE, Petry NA, Jaszczak RJ. Collimation for I-123 imaging with SPECT. In Esser PD, ed. *Emission computed tomography: current trends.* New York: Society of Nuclear Medicine; 1983:135–146.
6. Bolmsjo MS, Persson BRR, Strand SE. Imaging I-123 with a scintillation camera. A study of detection performance and quality factor concepts. *Phys Med Biol* 1977;22:266–277.
7. Clarke LP, Vaughan S, Hourani M, et al. Collimator choice for differential uptake measurements using SPECT imaging with I-123 [Abstract]. *J Nucl Med* 1983;24:P75.
8. Polak JF, English RJ, Holman BL. Performance of collimators used for tomographic imaging of I-123 contaminated with I-124. *J Nucl Med* 1983;24:1065–1069.
9. McKeighen RE, Muehllehner G, Moyer RA. Gamma camera collimator considerations for imaging I-123. *J Nucl Med* 1974;15:328–331.
10. Macey DJ, DeNardo GL, DeNardo SJ, Hines HH. Comparison of low- and medium-energy collimators for SPECT imaging with iodine-123-labeled antibodies. *J Nucl Med* 1986;27:1467–1474.
11. Kircos LT, Leonard PF, Keyes JW, Jr. An optimized collimator for single-photon computed tomography with a scintillation camera. *J Nucl Med* 1978;19:322–323.
12. Mueller SP, Polak JF, Kijewski MF, Holman BL. Collimator selection for SPECT brain imaging: the advantage of high resolution. *J Nucl Med* 1986;27:1729–1738.
13. Hanson KM. Variations in task and the ideal observer. *Proc SPIE* 1983;419:60–67.
14. Tsui BMW, Metz CE, Atkins FB, Starr SJ, Beck RN. A comparison of optimum detector spatial resolution in nuclear imaging based on statistical theory and on observer performance. *Phys Med Biol* 1978;23:654–676.
15. Tsui BMW. A correction to a comparison of optimum detector spatial resolution in nuclear imaging based on statistical theory and on observer performance. *Phys Med Biol* 1978;23:1203–1205.
16. Tsui BMW, Metz CE, Beck RN. Optimum detector spatial resolution for discriminating between tumour uptake distributions in scintigraphy. *Phys Med Biol* 1983;28:775–788.
17. Hoffman EJ, Phelps ME. Positron emission tomography: principles and quantitation. In: Phelps ME, Mazziotta JC, Schelbert HR, eds. *Positron emission tomography and autoradiography: principles and applications for the brain and heart.* Raven Press; 1986:281–284.
18. Phelps ME, Huang SC, Hoffman EJ, et al. An analysis of signal amplification using small detectors in positron emission tomography. *J Comput Assist Tomogr* 1982;6:551–565.